2022 21st International Symposium on Distributed Computing and Applications for Business Engineering and Science (DCABES)

Numerical simulation of particle interception efficiency on different fiber shapes

Xinyi Lin, Jingyue Wang*, Meiqing Wang
College of Mathematics and Statistics
Fuzhou University
Fuzhou, China
Email: 463776856@qq.com;
jingyuewang@fzu.edu.cn;
mqwang@fzu.edu.cn

Shumin Guo
School of Mathematical Science
Xiamen University
Xiamen, China
Email: shumin_guo@xmu.edu.cn

Gaofeng Zheng
Department of Instrumental and Electrical Engineering
Xiamen University
Xiamen, China
Email: zheng_gf@xmu.edu.cn

Choi-Hong Lai
Department of Mathematics
University of Greenwich
London, UK
Email: C.H.Lai@greenwich.ac.uk

***Abstract*—We use the Multiple-Relaxation-Time Lattice Boltzmann model to simulate the flow field and particle motion in a 2D porous media configured with various fiber cross-section shapes. Four sets of experiments are conducted to investigate the particle interception efficiency of four fiber structures with the same porosity. We find that: (1) with the same porosity, the filtration efficiency of hexagonal fibers is higher than that of fibers in other tested shapes; (2) sparse structures as shown in the ellipse and rectangular cases yield low filtration efficiencies even with a low porosity number.**

***Keywords*-the Multiple-Relaxation-Time Lattice Boltzmann model; particle interception efficiency; porosity.**

I. Introduction

In recent years, the use of nanofibers to construct efficient air filtration membranes sees more and more applications in fields such as mask designing, indoor air filtration system building, et al. The filtration mechanism of an air filtration membrane can be viewed as a two-phase flow problem on a porous medium composed of fibers. The air (air phase) flows through the porous medium, carrying solid particles (particle phase) forward. Solid particles are adsorbed by the medium during the process of transport to get filtered out. Filtration efficiency and pressure drop can be calculated in this process to indicate the filtration performance of the porous medium. The higher the filtration efficiency and the smaller the pressure drop, the better the filtration performance.

A characteristic quantity called porosity of materials is often correlated with the performance of filtration. High porosity typically leads to a low filtration efficiency combined with a low pressure drop, whereas low porosity typically leads to the opposite. Establishing the quantitative relationship between the porosity and the filtration efficiency can provide insights into the optimal design of efficient filter membrane. Moreover, it is interesting to investigate the influence of the geometry of the porous medium on particle interception rate which can help to accurately simulate and predict its filtration performance.

We use the lattice Boltzmann method to compute the fluid field. It is a mesoscopic method that can be applied in areas such as porous media, crystal growth that are difficult for traditional simulation methods to implement. The lattice Boltzmann method has inherent parallelism, as well as the advantages of simple boundary handling and easy implementation [1]. At present, extensive studies have been made on using the lattice Boltzmann method (LBM) to simulate the gas-solid two-phase flow in filtration [2–4].

Masselot and Chopard [5] are among the first to propose a CA probabilistic model that describes the motion of particles in a study on fiber filtration. Wang H, Zhao H [6, 7] et al. extended their work to simulate the movement process of particles under fibrous filters of different shapes.

In this paper, we use the lattice Boltzmann method to simulate the flow field in a porous media, and investigate the influence of different fiber shapes on particle interception efficiency in two-dimensional space. The paper is organized as follows. In Sec.2 we introduce the basic concepts of the lattice Boltzmann method and our particle trajectory model. In Sec.3 we present our numerical simulation, analyze and compare the influence of various geometric shapes on the filtration efficiency.

II. Prerequisites

A. Lattice Boltzmann method

1) Multiple-Relaxation-Time Lattice Boltzmann for Fluid Flow:

With the lattice Boltzmann method, the space-time is discretized into a regular grid of nodes. Moreover, the phase space at each node is also discretized into a finite number of directions, represented by the links connecting to the node. A discretized distribution function on position and velocity is defined on the grid.

The discrete velocity model used in LBM is often referred to as DdQm (d for dimensions, m for the number of discrete velocities) proposed by Qian [8] et al. This

2473-3636/22/$31.00 ©2022 IEEE
DOI 10.1109/DCABES57229.2022.00046

article uses a two-dimensional space D2Q9 model, as shown in Figure 1, where $\mathbf{c_i}, i = 1, \ldots, 9$ represent the direction of discrete velocity.

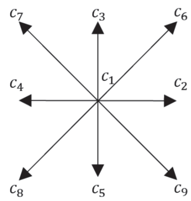

Figure 1. D2Q9 model

The weight factors for the nine velocity directions under the D2Q9 model are $\omega = \left\{ \frac{4}{9}, \frac{1}{9}, \frac{1}{9}, \frac{1}{9}, \frac{1}{9}, \frac{1}{36}, \frac{1}{36}, \frac{1}{36}, \frac{1}{36} \right\}$.

The evolution process of fluids, this paper will use the more widely used LB model – MRT model [9]:

$$\begin{aligned} f_i\left(\mathbf{x}+\mathbf{c_i} \cdot \Delta t, t+\Delta t\right)-f_i\left(\mathbf{x}, t\right) \\ =-S\left[f_i\left(\mathbf{x}, t\right)-f_i^{eq}\left(\mathbf{x}, t\right)\right] \end{aligned} \tag{1}$$

where $\mathbf{x}$ is the coordinate vector, i is the direction; $\mathbf{c_i}$ is the velocity vector in the ith direction at that position; Δt is the time interval; $f_i\left(\mathbf{x}, t\right)$ refers to the fluid particles' density distribution function, which at t-time, $\mathbf{x}$ position, in the ith direction, the velocity is $\mathbf{c_i}$; $f_i^{eq}\left(\mathbf{x}, t\right)$ is the equilibrium distribution function of the corresponding position and direction, and S is the collision matrix [8].

The above evolutionary equation can be divided into two parts, collision and streaming, which are calculated in two steps:

Collision:

$$f_i^{'}\left(\mathbf{x}, t\right)=-S\left[f_i\left(\mathbf{x}, t\right)-f_i^{eq}\left(\mathbf{x}, t\right)\right] \tag{2}$$

Streaming:

$$f_i\left(\mathbf{x}+\mathbf{c_i} \cdot \Delta t, t+\Delta t\right)=f_i^{'}\left(\mathbf{x}, t\right) \tag{3}$$

2) boundary condition:

Boundary condition is an important part of the implementation of the lattice Boltzmann method. In each step of collision, although the distribution function on the internal flow field node is available after each iteration, the particle distribution function on the boundary nodes is still unknown. Particle distribution functions on the boundary must be determined before the next calculation can be performed. This process is called the boundary processing scheme of the lattice Boltzmann method. In this paper, we use the periodic boundary condition that is often applied to periodic changes in fluid space or infinity in one direction. Periodic boundary condition reflects the fact that when fluid particles leave the fluid region from one boundary, they enter the original fluid region from another boundary at the next moment.

The schematic diagram with periodic boundary condition of a laminar flow on an infinitely long straight circular tube, called Poiseuille flow is shown in Figure 2.

The fluid nodes and the virtual fluid nodes to be added outside the fluid area are represented by solid

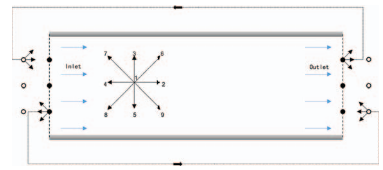

Figure 2. Schematic diagram of period boundary conditions

and dashed spheres respectively. We use a uniform grid $(i = 1, \ldots, n; j = 1, \ldots, n)$ to cover the fluid region, the X direction adopts the periodic boundary condition. Two layers of mesh $(i = 0,\ j = 1, ..., n)$ are added outside the fluid region in this direction; $(i = n+1,\ j = 1, ..., n)$ to represent virtual nodes. The distribution functions on the boundary are

$$f_{2,6,9}\left(0, j\right)=f_{2,6,9}\left(n, j\right) \tag{4}$$

$$f_{4,7,8}\left(n+1, j\right)=f_{4,7,8}\left(1, j\right) \tag{5}$$

B. Particle trajectory equation

Typically, aerosol particle captured by fibers in a porous media is influenced by inertial collisions, gravity, electrostatics, and Brown random diffusion. In this paper we consider only the inertial effects and electrostatic forces in fiber-trapped particles. The equation for particle motion is given by [10]

$$\begin{cases} \frac{d\mathbf{u}_p^*}{dt}+\mathbf{F_e}=\gamma\left(\mathbf{u}^*-\mathbf{u_p^*}\right) \\ \frac{d\mathbf{x_p}}{dt}=\mathbf{u_p^*} \end{cases} \tag{6}$$

where $\mathbf{u_p^*}$ is the particle velocity, $\mathbf{x_p}$ is the particle displacement, $\mathbf{u}^*$ represents the fluid vector velocity at the position of the solid particle, $\mathbf{F_e}$ is the electrostatic force between the fiber and the particle, and the γ coefficient is given by

$$\gamma=\frac{3\pi\mu D_p}{C_u \cdot M_p} \tag{7}$$

where μ is the dynamic viscosity, D_p is the particle diameter, C_u is Cunningham correction, and M_p is the particle mass.

In this paper, equation (6) is solved by explicit Euler's method to obtain the velocity and displacement of the particle:

$$\begin{cases} \mathbf{u_p^*}\left(x_p, y_p, t+1\right)=\Delta t \cdot \gamma \cdot \mathbf{u}^*\left(x_p, y_p, t\right)+... \\ \left(1-\Delta t \cdot \gamma\right) \cdot \mathbf{u_p^*}\left(x_p, y_p, t\right)-\Delta t \cdot \mathbf{F_e}\left(x_p, y_p, t\right) \\ \mathbf{x_p}\left(t+1\right)=\mathbf{x_p}(t)+\Delta t \cdot \mathbf{u_p^*}\left(x_p, y_p, t+1\right) \end{cases} \tag{8}$$

where x_p and y_p are the two directional components of the particle displacement $\mathbf{x_p}$, $\mathbf{u_p^*}\left(x_p, y_p, t\right)$ represents the velocity of the particle at (x_p, y_p) at the t-time, $\mathbf{u}^*\left(x_p, y_p, t\right)$ represents the velocity of the fluid at the particle position (x_p, y_p) at the t-time, and $\mathbf{F_e}\left(x_p, y_p, t\right)$ indicates the total combined force of the particle at (x_p, y_p) by the fiber static force in the system.

III. Numerical simulation

A. Fiber shape arrangement

In theoretical analysis, it is usually assumed that fibers are uniformly arranged in structure, and have a certain periodicity. Since this article mainly studies the effect of fiber shape on filtration efficiency, the fiber arrangement position is fixed. Cylindrical fibers with circular cross-section are the first shape considered in the study of filtration processes. We give a schematic diagram of the staggered arrangement model of cylindrical fibers, as shown in Figure 3:

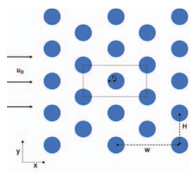

Figure 3. Schematic diagram of staggered cylindrical fiber arrangement model

In recent years, fiber cross-section is not limited to circular shapes. Many researchers have begun to study filtration process for non-circular fiber structures. With the same porosity non-circular fibers can have larger upwind contact surface area than circular fibers, therefore they may be more advantageous in terms of filtration efficiency [11]. In this paper, we carry out numerical experiments on fibers with various cross-section shapes in order to explore the influence of fiber geometry on filtration efficiency. The specific shapes are shown in Figure 4:

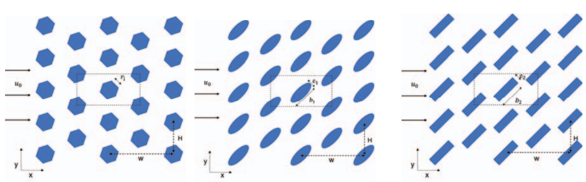

(a) (b) (c)

Figure 4. The schematic diagram of three specific shapes, (a) hexagonal fiber staggered arrangement model; (b) $\angle 45°$ elliptical fiber staggered arrangement model;(c) $\angle 45°$ rectangular fiber staggered arrangement model.

Among them, r_1, r_2 are the radius of the circle and the side length of the regular hexagon, respectively, a_1, b_1, a_2, b_2 are the lengths of the long and short sides of the ellipse and the rectangle, respectively. W, H refer to the pitches of the parallel and vertical directions of fluid flow respectively. The dashed rectangles in the four pictures represent the corresponding representative elementary volumes (REVs). Here, the fiber shape and size are the same for each structure, so only the porosity and solid volume fraction of the fiber structure need to be determined from each REV.

B. Parameter settings

1) Porosity φ:

Porosity is defined by the ratio of pore volume to total volume:

$$\varphi = \frac{volume\ of\ Pore}{total\ \ volume} \tag{9}$$

Its value is between 0 and 1. Porosity is one of the factors that in combination determine the hydraulic conductivity of materials.

2) solid volume fraction β:

The solid volume fraction is defined by the ratio of the volume of the fiber structure to the total volume. Its relationship with the porosity is:

$$\beta = 1 - \varphi \tag{10}$$

The porosity φ and the solid volume fraction β of the four fiber structures in Subsection (A) are calculated and displayed in Table I:

Table I
Porosity and solid volume fraction of four fiber structures

parameter / Fiber structure	Solid volume fraction β	Porosity φ
Circular section	$\beta_c = \frac{\pi r_1^2}{WH}$	$\varphi_c = 1 - \frac{\pi r_1^2}{WH}$
Hexagonal Section	$\beta_h = \frac{3\sqrt{3}r_2^2}{4WH}$	$\varphi_h = 1 - \frac{3\sqrt{3}r_2^2}{4WH}$
Ellipse section	$\beta_e = \frac{\pi a_1 b_1}{WH}$	$\varphi_e = 1 - \frac{\pi a_1 b_1}{WH}$
rectangular section	$\beta_r = \frac{a_2 b_2}{WH}$	$\varphi_r = 1 - \frac{a_2 b_2}{WH}$

3) Filtration efficiency η:

Filtration efficiency is defined by the ratio of the number of particles intercepted by the filter to the number of particles contained in the fluid (air) before filtering, the specific formula is:

$$\eta = \frac{The\ number\ of\ particlesintercepted\ by\ the\ filter}{The\ number\ of\ all\ particlescontained\ in\ the\ inflow\ fluid} \tag{11}$$

This article will adjust the size of the individual fibers to ensure that the four fiber configurations in experiments have the same volume.

C. Experimental results

We assume that the filtration process satisfies the following conditions: (1) the fluid is steady, laminar and incompressible; (2) particles enter the computing area from the inlet, and as long as they collide with the fibers in movement, they are adsorbed; (3) particles are adsorbed on a fiber without affecting the fiber size; (4) when a particle reaches the outlet, it is considered an escaped one.

Parameter setting:

Table II
Parameter setting

Fiber structure / porosity	circle	hexagon	ellipse	rectangle
$\varphi = 55\%$	$r_1 = \frac{3}{50}\sqrt{\frac{5}{\pi}}$	$r_2 = \frac{\sqrt{10\sqrt{3}}}{50}$	$a_1 = \frac{3}{25}\sqrt{\frac{5}{\pi}}, b_1 = \frac{3}{100}\sqrt{\frac{5}{\pi}}$	$a_2 = \frac{3\sqrt{10}}{50}$, $b_2 = \frac{3\sqrt{10}}{100}$
$\varphi = 59.5\%$	$r_1 = \frac{9}{100}\sqrt{\frac{2}{\pi}}$	$r_2 = \frac{3\sqrt{\sqrt{3}}}{10}$	$a_1 = \frac{9}{50}\sqrt{\frac{2}{\pi}}$, $b_1 = \frac{9}{200}\sqrt{\frac{2}{\pi}}$	$a_2 = \frac{9}{50}, b_2 = \frac{9}{100}$

Experimental environment: We conduct numerical experiments on a machine with Ryzen 7 5800H and windows 11 operating system, the code is written in python.

In Figure 5, all fiber-particle configurations are set with 60 inlet particles and a porosity of 55%.

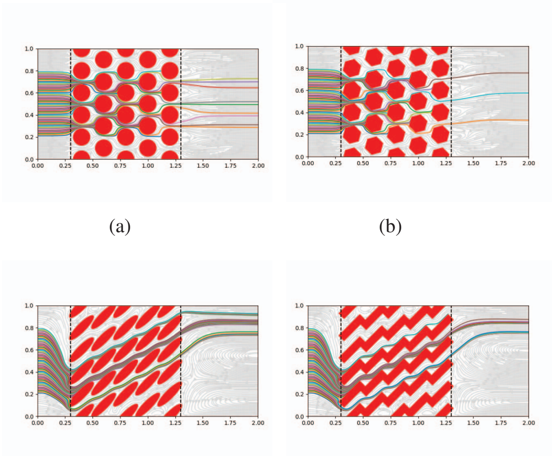

(a) (b)

(c) (d)

Figure 5. All fiber-particle configurations are 60 inlet particles with a porosity of 55%, (a) The effect of circular fiber intercepting particles; (b) The effect of hexagonal fibers intercepting particles;(c) The effect of $\angle 45°$ elliptical fiber intercepting particles; (d) The effect of $\angle 45°$ rectangular fiber intercepting particles.

We show filtration efficiency results obtained from numerical simulation for the four fiber configurations in Table III. For each configuration, two data points with particle number 60 and 100 respectively are collected.

Table III
FILTRATION EFFICIENCY OF FOUR FIBER STRUCTURES UNDER DIFFERENT POROSITY

Fiber structure / parameter	circle	hexagon	ellipse	rectangle
n=60, $\varphi = 55\%$	85%	95%	3.3%	40%
n=60, $\varphi = 59.5\%$	60%	73%	5%	5%
n=100, $\varphi = 55\%$	87%	96%	3%	40%
n=100, $\varphi = 59.5\%$	60%	72%	2%	7%

We find in the numerical simulation that the efficiency of hexagon-shaped fibers is always higher than that of other shapes. Filtration efficiencies for circular and hexagonal fibers are decreasing when the porosity increases. On the other hand, rectangular and elliptic fibers yield very low filtration efficiencies. This is mainly due to the wide empty channels with an orientation of 45° formed in the filtration region as shown in Figure 5(c) and Figure 5(d). Most particles leaked through these channels.

CONCLUSION

In this paper, we use the Multiple-Relaxation-Time Lattice Boltzmann method to simulate a laminar air flow with submicron particles in a porous media, where various regularly shaped fiber cross-sections are set in a uniform structure. Four fiber configurations are tested. In our numerical experiments, only hydrodynamic theory and electrostatic force are considered. We observe that regular hexagon shaped fiber cross-section has a minor but decisive advantage over circle shaped cross-section in filtration efficiency in all experiment settings. We also observe that the other two configurations with rectangle and ellipse shaped cross-sections exhibit large empty channels in the penetration region, resulting in low filtration efficiency. This implies that in designing new fiber structures, geometric configuration in addition to porosity should be taken into account to improve the overall filtration efficiency.

IV. ACKNOWLEDGMENT

This work was supported in part by the National Natural Science Foundation of China under Grant 11771084; in part by the Fujian Provincial Department of Science and Technology under Grant 2020H6003.

REFERENCES

[1] He Y, Wang Y, Li Q. Lattice Boltzmann Method: Theory and Applications[M]. China Science Publishing, 2009. (in Chinese)

[2] Wang H, Zhao H, Guo Z, et al. Simulation of Particle Capture Process for Elliptical Fibers by Lattice-Boltzmann Two-phase Flow Model[J]. Proceedings of the CSEE, 2013, 33(8): 50-57. (in Chinese)

[3] Filippova O, Hänel D. Lattice-Boltzmann simulation of gas-particle flow in filters[J]. Computers and Fluids, 1997, 26(7): 697-712.

[4] Fang Xin, Li Shanhong, et al. Numerical simulation of gas-solid two-phase flow on dust collection filters using Lattice Boltzmann Method[J]. Chinese Journal of Environmental Engineering, 2013, 7(5): 1883-1888.

[5] Masselot A, Chopard B. A lattice Boltzmann model for particle transport and deposition[J]. EPL (Europhysics Letters), 1998, 42(3): 259.

[6] Wang H, Zhao H, Guo Z, et al. Numerical simulation of particle capture process of fibrous filters using Lattice Boltzmann two-phase flow model[J]. Powder technology, 2012, 227: 111-122.

[7] Wang H, Zhao H, Guo Z, et al. Lattice Boltzmann method for simulations of gas-particle flows over a backward-facing step[J]. Journal of Computational Physics, 2013, 239: 57-71.

[8] Qian Y H, d'Humières D, Lallemand P. Lattice BGK models for Navier-Stokes equation[J]. EPL (Europhysics Letters), 1992, 17(6): 479.

[9] Krüger T, Kusumaatmaja H, Kuzmin A, et al. The lattice Boltzmann method[J]. Springer International Publishing, 2017, 10(978-3): 4-15.

[10] Kerner M, Schmidt K, Hellmann A, et al. Numerical and experimental study of submicron aerosol deposition in electret microfiber nonwovens[J]. Journal of Aerosol Science, 2018, 122: 32-44.

[11] Zhu C., Lin C.H., Cheung C.S. Inertial impaction-dominated fibrous filtration with rectangular or cylindrical fibers[J]. Powder Technology, 2000, 112(1): 149-162.